NASA MARSHALL SPACE FLIGHT CENTER
RESEARCH GRANT NO NAG 8005
FINAL TECHNICAL REPORT

A TEST AND INSTRUMENTATION SYSTEM FOR THE INVESTIGATION OF DEGRADATION OF ELECTRICAL INSULATING MATERIALS

SUBMITTED BY

C. V. Doreswamy
Professor of Electrical Engineering
School of Engineering
Tuskegee Institute
Tuskegee Institute, AL 36088

January, 1982

NASA MARSHALL SPACE FLIGHT CENTER
RESEARCH GRANT NO NAG 8005
FINAL TECHNICAL REPORT

A TEST AND INSTRUMENTATION SYSTEM FOR THE INVESTIGATION OF DEGRADATION OF ELECTRICAL INSULATING MATERIALS

SUBMITTED BY

C. V. Doreswamy
Professor of Electrical Engineering
School of Engineering
Tuskegee Institute
Tuskegee Institute, AL 36088

January, 1982

ABSTRACT

Electrical insulating materials used on spacecraft systems deteriorate due to effects of thermal cycling, very high electric fields, partial discharges due to corona and electrical discharges initiated by space plasma interaction.

This report briefly discusses the basic test methods of aging and deterioration mechanisms of electrical insulating materials.

A comprehensive test system developed to study the degradation process is described. This system is completely checked, and calibrated with a few insulating material samples. However, no complete test results and conclusions of test results are presented due to non-availability of sufficient number of test samples to analyze the results using the Standard Statistical Methods.

CHAPTER I

INVESTIGATION OF DEGRADATION PROCESS OF INSULATING MATERIALS

Introduction

The prevention of degradation of Electrical Insulation and prevention of breakdown in flight and spacecraft systems have been a major topic of numerous studies conducted by NASA and other agencies (1,2,3,4,5,6).

The primary causes of deterioration of the electrical insulation are:

(1) Thermal cycling and extreme high temperatures;

(2) Internally generated space charge effects, primarily due to corona. Corona usually originates at very high electric fields resulting in the ionization and breakdown of the dielectric (gas). The free electrons and ions generated due to corona are accelerated in the presence of a high electric field acquiring sufficient energy to cause structural damage to the molecules and destroy the insulating properties;

(3) High energy radiation due to natural causes. Ultraviolet and cosmic radiations.

(4) Space plasma interaction with solar cell arrays.

The problems of spacecraft charging and plasma initiated discharges become very critical in case of high voltage Solar-cell arrays required in plasma engines for spacecraft propulsion

systems. Numerous studies have been conducted by NASA and other agencies to explore these problems (7,8,9,10,11,12). However, it was suggested that there is no single universal solution to this problem (8).

From these investigations it has been found that the elements which bring about the degradation and catastrophic breakdown include the chemical changes in the insulating materials brought about by electrical discharges - which may be initiated either by plasma or corona discharges at the points of very high electrical stresses.

The short term breakdown of the material is usually a result of a high voltage surge, which might occur either due to an external cause like lightning, or electrostatically induced surges or malfunction of the high voltage supply which might cause a switching surge severe enough to destroy the insulation and the system.

The long term breakdown of the material occurs gradually (a period of weeks or hours) due to partial discharges at the points of high electrical stress. These points of high electrical stress typically occur at the discontinuity of the dielectric material like voids, holes and other microscopic manufacturing imperfections. Partial discharges and corona

which create high energy ions interact with the molecular structure of the insulating material leading to a breakdown (4).

Additionally, the breakdown of the insulation occurs also due to thermal processes. The heat generated due to ohmic losses in the conductor and dielectric losses in the insulating materials are the main causes for this type of thermal deterioration and breakdown (3,11).

There is a great need for further intensive investigation of these degradation processes.

This report describes the test systems developed for the extensive experimental investigation to study the effect of thermal stresses, electrical fields, and corona discharges on Electrical Insulating materials

CHAPTER II

PROPERTIES OF ELECTRICAL INSULATING MATERIALS

Electrical insulating materials, which are also known as dielectric materials, isolate components of the electrical system from one another and from the ground. They also provide mechanical support for the components. The term dielectric is used when the insulating material is used for storage of electrical charges. A typical device for the storage of electrical charge is a capacitor.

Insulating Material Under Constant (D.C.)Voltages

When a D.C. voltage is applied to a perfect insulating material, no ohmic current will flow through the material. However, a small current will flow through the practical insulating materials. Only a perfect vacuum is a perfect insulator.

Two parameters characterize the behavior of the insulating material with D.C. voltages:

Volume Resistivity

Volume resistivity of the material is the ratio of the potential gradiant parallel to current in the material to the current density.(19) The volume resistivity of the

insulating material is dependent on the density of the charge carriers - electrons and ions per unit volume - in the material and the ease of moving these charged particles through the insulating materials under the applied voltage. Both the magnitude of the voltage and the temperature affect the charge transport through the material.

Surface Resistivity

Surface resistivity of a material is the ratio of the potential gradiant parallel to the current along its surface to the current per unit width of the surface (19). Surface resistivity of a material is numerically equal to the surface resistance between two electrodes forming the opposite sides of a square. The size of the square is immaterial. ASTM Standard D257-66 specifies the test methods and the electrode systems for measuring D.C. surface and volume resistivities. The complete test system for these measurements is described in Chapter V of this report.

Insulating Material Under Alternating Voltage Conditions

The behavior of a dielectric in an alternating current field can be represented by means of a Complex dielectric permittivity.

$$\varepsilon = \varepsilon' - j\varepsilon''$$

The dielectric can be schematically represented by a combination of a perfect capacitor and a resistance as shown in Fig (1). Only a perfect vacuum is a perfect dielectric and can be represented by a capacitor alone.

The power dissipated in the capacitor due to dielectric losses is given by

$$P = V^2 \omega c \tan\delta$$

$\tan\delta$ is called the dissipation factor of the dielectric and δ is known as the loss angle of the dielectric. Fig 1(c) shows the phasor diagram defining the angle δ.

It can be shown that

$$\tan\delta = \frac{\varepsilon''}{\varepsilon'}$$

The dielectric losses in the insulating materials are caused by various polarization mechanisms that occur inside the material when an electrical field is applied. In general, both ε' and ε'' are dependent upon temperature, frequency, and applied electrical field. The measurement of the variation of the value of $\tan\delta$, with voltage, temperature and frequency enables one to deduce the dynamics of molecular interactions. The value of the dissipation factor is a measure

of the heat generated in the material and must be held small. Dissipation factor is used to indicate the quality of the insulating material with other correlating data characterizing the insulating material.

Dielectric loss index is defined as

$$\varepsilon'' = \varepsilon' \tan\delta$$

Series & Parallel Equivalent Circuits of Capacitor with Dielectric Losses

Fig 1 (a,b) show the equivalent circuits of a lossy capacitor and Fig 1 (c,d) show phasor diagrams corresponding to these equivalent circuits.

The dissipation factor of the parallel circuits is defined as:

$$\tan\delta_p = I_{r/I_c} = \frac{1}{\omega C_p R_c}$$

and that of the series equivalent circuit

$$\tan\delta_s = \frac{V_r}{V_c} = R_s \omega c_s$$

Series Circuit **Parallel Circuit**

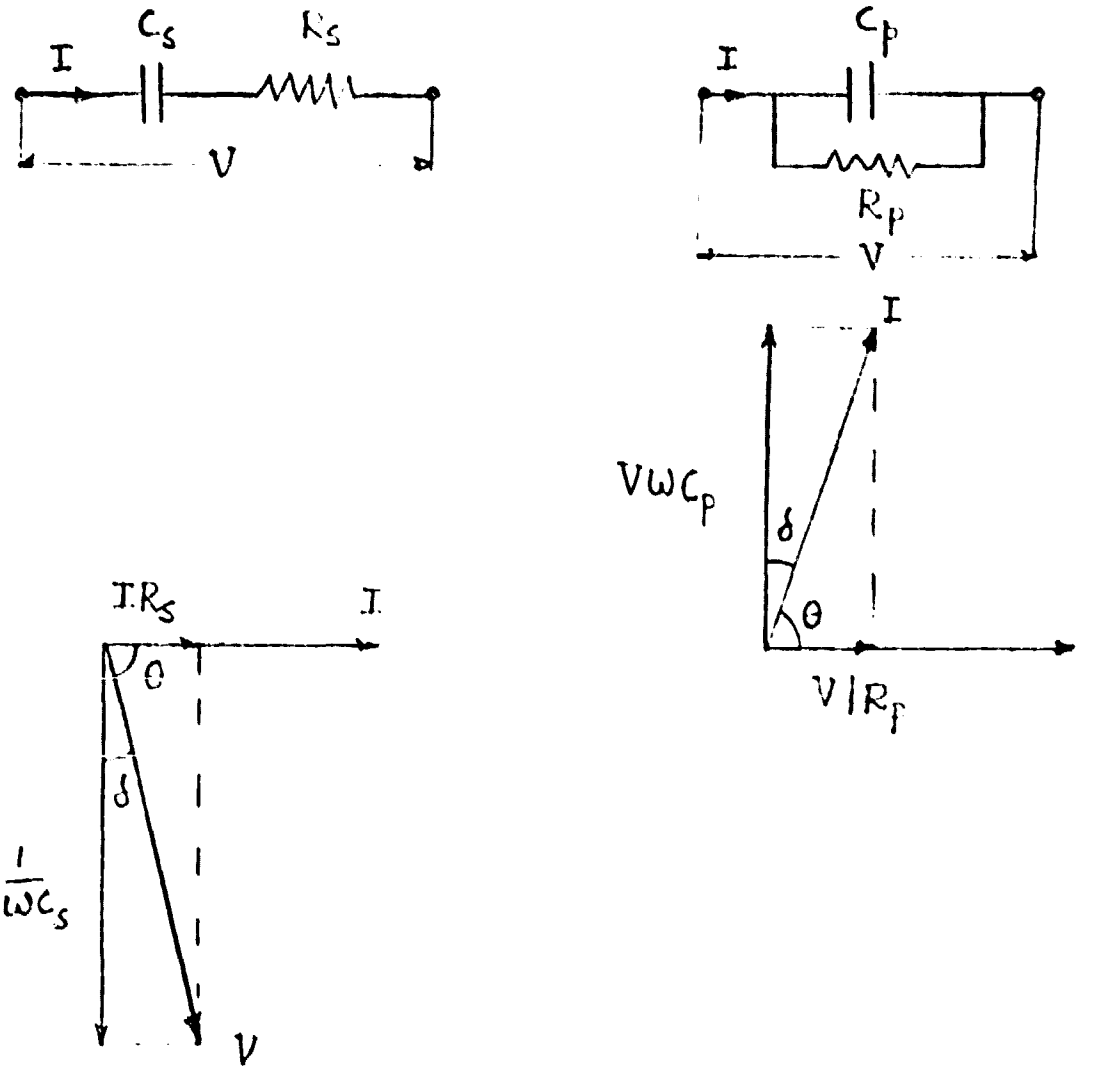

Phasordiagrams

Fig (1) Equivalent Circuit of a Lossy Capacitor.

In general, a capacitor possesses both the series and parallel loss resistance as shown in Fig (2). Depending on the frequency of the applied voltage, only one of them dominates. In Fig (2), R_s represents the resistance of the connecting leads, electrode contact resistances and the part of the dielectric loss whose characteristics can be more accurately described by a series equivalent circuit.

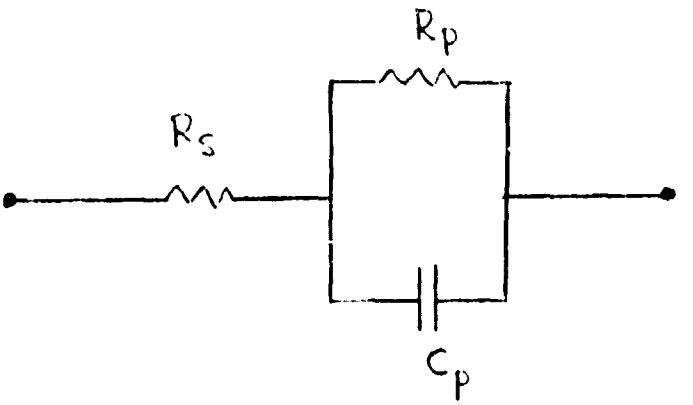

Fig (2)

Resistance R_p represents a measure of the dielectric losses inside the material. At low frequencies $\frac{1}{\omega C_p} >> R_s$ and only

parallel circuit is effective.

At high frequencies, the losses are mainly determined by R_s. However, at any particular frequency both the circuits are accurate. But over a wide frequency range, either of the circuits alone is inaccurate.

The relation between series and parallel equivalent resistance and capacitances are given by:

$$R_p = R_s\ (1 + 1/\tan^2\delta) \qquad C_p = C_s/(1 + \tan^2\delta)$$

$$R_s = R_p/(1 + 1/\tan^2\delta) \qquad C_s = C_p\ (1 + \tan^2\delta)$$

The equivalent converted values are valid for only one frequency because the dissipation factor $\tan\delta$ itself is frequency dependent.

The values of ε', ε'' and $\tan\delta$ with frequency and temperature can be examined further by examining the polarization phenomena of the dielectric material.

POLARIZATIONS

The difference between the permittivity of a dielectric and the permittivity of free space is due to the restricted elastic movements of the charges within the dielectric. Positive charges and negative charges move oppositely under the influence of an external electric field. There is no net

charge anywhere in the dielectric, but there is a positive charge at the surfaces where the direction of the electric field emerges and a negative charge at the surface where the field enters, as shown in Fig (3). This production of the electric field within the dielectric due to restricted motion of bound charges is called polarization

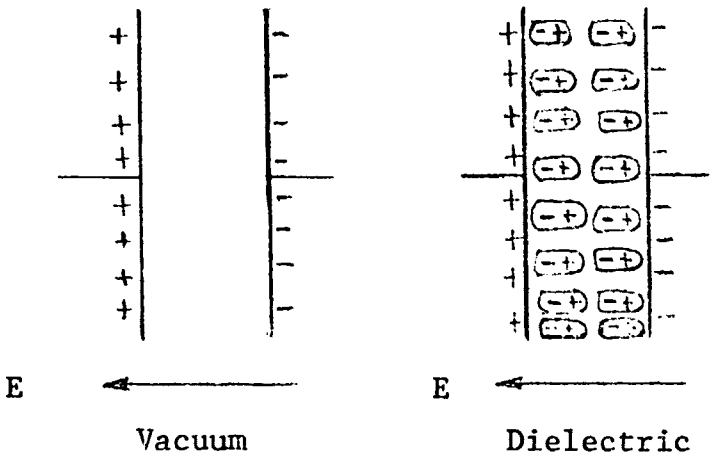

Fig (3)

The polarization generally consists of four basic kinds: electronic, atomic, dipole and interfacial polarizations.

(a) Electronic polarization is the displacement of electrons with respect to the atomic nucleus under the action of an external electric field. This type of polarization occurs in all atoms and ions. The polarization takes place in a very short time of the order of 10^{-15} seconds;

(b) Atomic polarization is the mutual displacement of ions in an ionic crystal or atoms in a molecule. The time required for polarization to set in is larger than that required for electronic polarization. The displacement of heavier atoms requires more time in the order of 10^{-12} to 10^{-13} seconds;

(c) Dipole polarization or orientational polarization arises due to rotation or orientation of the molecules of a polar dielectric having a constant dipole movement in the direction of the electric field. The time of establishing the dipole polarization can be very large - which may be in the order of seconds, microseconds, or nanoseconds (22).

(d) Interfacial polarization is due to charge carriers (both electrons and ions) and not bound charges. The polarization occurs when the charges accumulate at the interfaces in the phases of a heterogeneous material when they differ each other in permittivity ϵ' and AC conductivity.

The total polarization is the sum of all the four additive components described above.

The polarization vector in a material is equal to dipole movement per unit volume of the material

$$P = (\epsilon' - \epsilon_o)E \qquad Col/m^2$$

Relative dielectric constant k' is related to the polarization vector P and the applied electric field E.

$$P = (k' - 1)\,\epsilon_o E$$

where ϵ_o = permittivity of free space

k' = Relative dielectric constant

If an alternating voltage is applied to a dielectric system, it will be necessary for the direction of polarization to reverse each time the polarity of the electric field changes. The speed with which the polarity can change depends, among others, upon the mass of the charge carrier and the viscosity of the dielectric as determined by the molecular structure. If the frequency of the applied voltage becomes so high that the polarization does not have time to form, then the contribution of this particular kind of polarization to the net value of the dielectric constant will disappear. This leads to a frequency dependence of the dielectric contact (23).

The real part of the complex permittivity ϵ' will decrease through

the value $\omega_o = 1/\tau$ is called the relaxation time. There is an increase in the dielectric loss factor ε'' and passes through the maximum value at frequency ω_o. At frequencies $\omega < \frac{1}{\tau}$, ε'' will be much smaller than its maximum value at Fig (4) shows the variation of ε' and ε' with the frequency.

Dependence of Permittivity and tanδ on Various Factors

The dielectric constant of the material depends on changeable external factors, such as frequency, temperature, humidity, corona, etc.

Frequency The time required for electronic and ionic polarization to set in is very small when compared to the time of the voltage reserval (half period of an A.C. voltage) even at the highest frequencies used in electric power and communication equipment. The polarization establishes itself completely in one half period of the applied voltage wave. The dielectric constant is hence essentially independent of the frequency for non-polar materials. For polar materials, the change in the real and imaginary parts of the dielectric constant is expressed by Debye equations. One version of the Debye equations which may be written in various forms is (20).

$$\epsilon' = \epsilon_i + (\epsilon_s - \epsilon_i)/(1 + \omega^2 \tau^2)$$

$$\epsilon'' = (\epsilon_s - \epsilon_i)/(1 + \omega^2 \tau^2)$$

in which:

ϵ_i = Initial value of the permittivity due to electronic polarization.

ϵ_s = Final Value of the permittivity after the dipole polarization has completely set in.

τ = Relaxation time.

$\omega = 2\pi f$ = Angular frequency of the applied A.C. voltage.

$\tan\delta = \epsilon''/\epsilon'$

ϵ'' approaches zero for small and large values of $\omega\tau$ and has a maximum for $\omega\tau = 1$.

At this value of ω

$$\epsilon'_m = (\epsilon_i + \epsilon_s)/2$$

and

$$\epsilon''_m = (\epsilon_s - \epsilon_i)/2$$

The value of ϵ' decreases from ϵ_s to ϵ_i within the increase in frequency.

Depending on the relaxation time and of the type of polarization - electronic, atomic or dipole - the maximum value of ϵ'' occurs at different frequencies as shown in Fig (4).

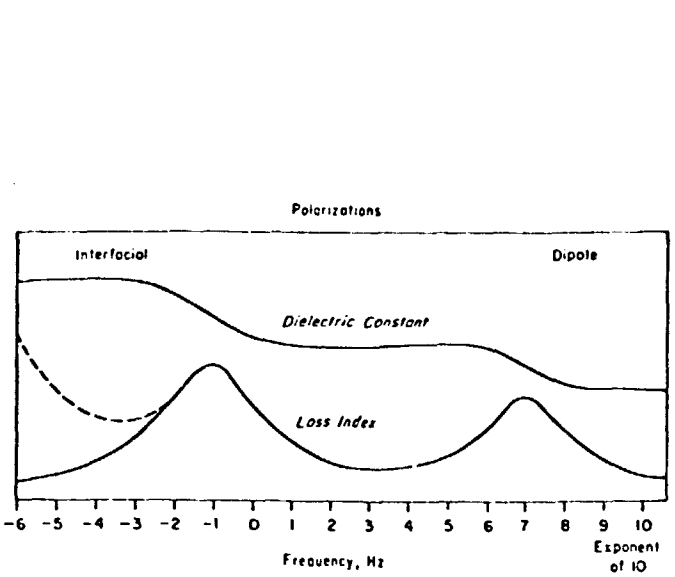

Fig (4) Polarizations

The relaxation time can be experimentally measured by observing the frequency ω_m at which the dielectric loss factor is a maximum. Then $\omega_m = 1/\tau$

Temperature

The major effect of the temperature on an insulating material is to increase the relaxation frequencies of its polarizations. In most cases, the increase in temperature facilitates the orientation of the dipoles thereby increasing the value of ε'. As the temperature grows, the chaotic thermal oscillations of molecules are intensified and the degree of orderliness of their orientation is decreased. The graph of ε' vs. temperature shows ε' reaching a maximum value and then decreasing with increase of temperature (22).

The temperature coefficient of the dielectric loss index may be positive or negative, depending on the relation of the measuring frequency to the relaxation frequency. It will be positive for frequencies higher than the relaxation frequency and negative for lower frequencies. At 60Hz, the temperature coefficient of dielectric loss index is positive (19).

As a general rule, $\tan\delta$ appreciably increases when temperature rises. Therefore, with the increase in $\tan\delta$, the insulation will operate under more strenuous conditions at high

temperatures. The increase of tanδ is brought about by an increase of both conduction and absorption currents.

The dielectric losses caused by the dipole mechanisms reach their maximum at a certain definite temperature. The rise in temperature and the resulting drop in viscosity exert opposite effect on the amount of losses due to friction of the rotating dipoles. On one hand, the degree of dipole orientation increases, thereby increasing the power loss and tanδ, whereas on the other hand reduction of viscosity decreases the energy dissipated when the dipole rotates through a unit angle, (22).

The polar substances or their mixtures with non-polar substances exhibit losses due to conduction in addition to dipole polarization losses. The conduction losses increase with the increase of temperature. The variation of tanδ with the variation of temperature is the sum of these losses and shown schematically in Fig (5).

A = Loss due to dipole polarization alone

B = Loss due to conduction alone

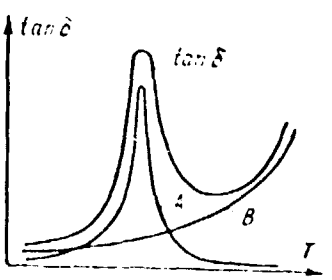

Fig (5)

Voltage

The value of tanδ does not appreciably depend on the applied voltage, so that all other conditions being equal the dielectric losses in the material increase in proportion to the square of the voltage. If this increased dielectric loss is not dissipated by cooling mechanisms, the temperature inside the dielectric material increases, thereby changing tanδ due to temperature effects. Thermal breakdown of the insulating material can occur under these conditions.

All dielectric polarizations except the interfacial are independent of the electric field in the material. The value of tanδ is practically a constant with the increase in the electric field until such a value is reached that the ionization occurs in voids in the material or on the surface. Any sudden increase in the value of tanδ indicates a local ionization and breakdown and will ultimately lead to total failure of the insulation. This ionization causes two effects:

(a) Considerable absorption of energy which increases the losses in the dielectric and hence tanδ;

(b) Formation of ozone and oxides of nitrogen which react with the molecules of the insulating material.

The resultant structural changes will gradually destroy the insulating properties.

The practical operating voltage of the insulating materials are as a rule less than the ionization voltage. Modern instrumentation makes it possible to detect even very small partial discharges.

CHAPTER IV

DEGRADATION AND AGING PROCESS OF INSULATING MATERIALS

The characteristics of the insulating material - namely, permittivity, tanδ, volume resistivity, and surface resistivities do not remain constant over a long period of time. They are changed by temperature, moisture, electrical stress, partial discharges and corona, and several other environmental factors. The quality of the insulating materials deteriorate as they age. Aging is the irreversible change in the properties of the insulating material in service under the action of several aging factors. IEC TC 63 defines aging as: "The irreversible deleterious change in the serviceability of insulations systems. Such changes are characterized by a failure rate which increases with time." A large amount of published data is available on the effects of various environmental factors on the aging process of insulating materials (16,24,25). However, there is a great divergence of views regarding the test, modeling and diagnostic methods to enable one to reliable prediction of the long-term behavior of the insulating material (25).

Thermal Aging

The thermal aging is generally described by the well-known Arrhenius equation. According to this theory, the rate of aging is proportional to the acceleration of the chemical reaction rate caused by the increase of temperature.

R_t = Aging Rate = A exp (-B/T)

A and B are constants.

$B = We/_k = \frac{\text{Activation energy}}{\text{Boltzs manns constant.}}$

T = Absolute temperature.

The life of an insulating material is the time from the start of the test to the moment the specimen is judged to have failed as indicated by a specified criterion - electrical or mechanical breakdown. In general, the life is inversely proportional to the aging rate

$LnL = A + BT$ L = Time to failure (Life)

The above relation indicates that the plot of logarithms of time to failure against the inverse of the absolute temperature ($1/_T$) is a straight line. Because of the scatter of the time to failure, statistical methods must be used to draw the "best" line. However, it should be noted that the above relation is based on the assumption that the aging rate progresses continuously and due to a single chemical reaction. (20)

Electrical Aging (Voltage Endurance)

The time to failure of an insulation system at constant temperature has been described by the well-known inverse power law (24).

$L = K/g^n$ = Time to failure (lifetime)

where g = electrical stress volts/meter.

K and n are constants dependent on temperature, other environmental effects and the characteristics of the material.

The following empirical formula relates the time to failure with corona inception gradients (21).

$$\left[(E - E_i)/E\right]^n t = C$$

where

E = applied field strength Volts/Mil

E_i = Corona inspection field strength Volts/Mil

t = time to breakdown hours.

Typcail experimentally determined values of E, n and c are listed below (5).

Material	E_i	n	c	Time t hours E = 500 V/mil.
Nylon	126	1.79	362	60 hr.
Mylar	296	1.52	22.4	50 hr.
Teflon	286	1.79	6.89	11 hrs.

The time to failure under combined temperature and

voltage stress is given by Simoni (24).

$$L = 1/A \exp\left(\frac{B}{T}\right) \exp -\left[\left(\alpha + \frac{b}{T}\right)G\right]$$

where A, B, α , b are constants independent of time, temperature and electric stresses.

T = absolute temperature

G = electrical gradient

CHAPTER V

TEST AND INSTRUMENTATION SYSTEM

Three important parameters are used to indicate the quality and stability of the insulating materials. They are:

(1) Amount of heat loss produced in the materials when subjected to alternating electrical fields. The measurement and analysis of mechanisms of loss production, enables us to deduce the dynamics of molecular interactions and the structural changes in the material. The dissipation factor of the material characterizes the heat loss produced.

(2) Dielectric breakdown and breakdown strength of the material. The dielectric breakdown tests are destructive tests and intended for use as a control and acceptance test. These tests are also used to ascertain the changes in the materials due to specific deteriorating causes.

(3) Surface and volume resistivity (conductivity) characteristics. Surface resistivity and volume resistivity can be used to predict the low frequency

dielectric breakdown and dissipation factor properties of some dielectric materials. These measurements are useful only if correlation can be established by supporting theoretical and experimental investigations.

To evaluate and experimentally investigate the changes in the quality and stability of the insulating materials, all the three above-mentioned quantities must be measured. The changes in the dissipation factor, dielectric strength, surface resistivity and volume resistivity must be correlated with the variation of temperature, voltage and corona intensity.

The test set up developed to subject the test samples to the effects of temperature cycling, corona and high electrical voltages is described in the succeeding sections of this report.

The test set up and measurements are primarily aimed at the measurement and analysis of the degradation of the electrical insulating properties of material used on Solar Cells. Degradation characteristics of the material subject to thermal cycling, space plasma and very high electrical fields individually and in combination can be investigated. Ultimate breakdown tests can be conducted using ASTM Standard Methods D149.

High Voltage Test Chamber

In order to investigate the variation of the important parameters that characterize the quality and stability of the insulating material, it is very essential that a test chamber be engineered to satisfy the following requirements:

(1) It should be possible to subject the insulating materials to thermal cycling between the operating temperatures of the Solar Cell Array;

(2) Provision must be made to inject corona and space charges onto the surface of the insulating material under investigation at various temperatures;

(3) It should be possible to conduct measurements of dissipation factor and breakdown voltage, with the best sample inside the chamber and at high voltages;

(4) The test chamber and associated equipment must not generate spurious signals or interferences which might render the measurements inaccurate.

An environmental chamber which can accomplish the requirements listed above has been constructed, with the following capabilities:

(1) The chamber is capable of providing and maintaining a desired test chamber temperature between the ranges of -100°F to +450°F;

(2) Provision has been also made to apply test high voltage to the material samples in the test chamber;

(3) Automatic temperature control devices and temperature measuring elements have been calibrated using standard methods of temperature measurement;

(4) As the test samples are of small physical dimensions, it will be assumed that the temperature at all points of the test sample is uniform and is indicated by the steady temperature of the test chamber. Any introduction of thermocouples or transducers in the electrode system will distort both the thermal and electrical stress fields, and hence is highly undesirable;

(5) It is essential that all the electrical supplies, connections and electrodes shall be corona free. The application of electric voltages shall not introduce any extraneous free charges - electrons or positive ions - into the test sample;

(6) To make certain that the requirement listed in (5) above is satisfactory, the test chamber with all the high voltage supplies was energized and tested up to 10 KV r.m.s., and found to be corona free. The discharge detection system is capable of detecting charges of 0.1 pico coulomb.

(7) Fig (6) shows the high voltage test set-up.

Low Voltage Test Cell

The low voltage test cell will complement the capabilities of the high voltage test chamber and will be used to conduct the following tests:

(1) Thermal cycling - from ambient to $150^{o}C$;

(2) Measurement of Capacitance and tanδ at 1000 Hz;

(3) Measurement of D.C. volume and surface resistivities.

It is possible to measure the capacitance, tanδ, and D.C. resistivities at various temperatures (max $150^{o}C$), and voltages (max. 2 kv D.C. under vacuum (10^{-3} Torr) or inert atmospheric (nitrogen) conditions.

This chamber will be used to conduct tests with the chamber filled with nitrogen. Additional tests will be also conducted in vacuum.

The chamber and the electrodes are manufactured by Tettex A.G., Zurich, Switzerland.

Fig (7a) shows the test set-up to measure tanδ and capacitance at 1000 Hz. (7b) shows the details of the low voltage electrode system and the test cell.

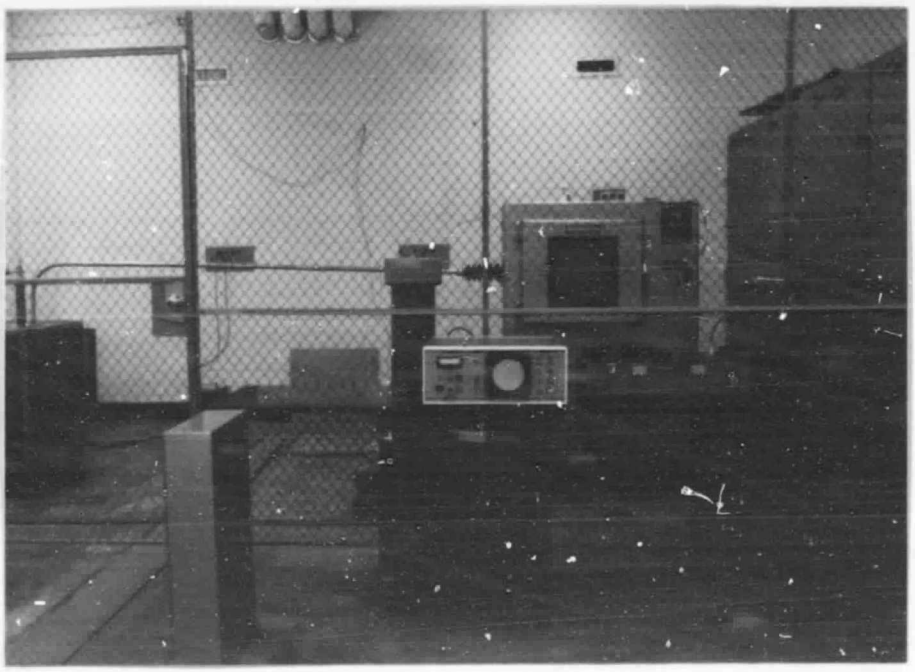

Fig (6) High Voltage Test Set Up

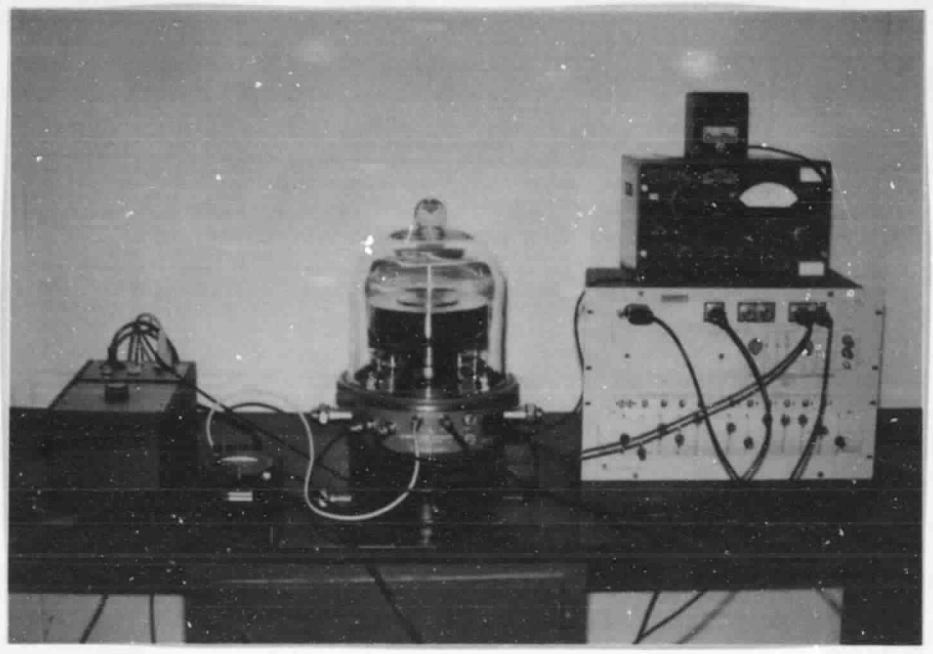

Fig (7)(a) Low Voltage Test Cell, with temperature control and capacitance bridge.

3. Type 2904 guard-ring capacitor (measuring cell for paper)

A. Principal data

Plate capacitor conforming to VDE 0311 and 0345 with guard-ring, used as cell for measuring solid insulating materials, e.g. cable and capacitor papers, etc.

Electrode surface area	20 cm^2 (diam. 49.5 mm)
Electrode pressure	min. 20 g/cm^2
	max. 1000 g/cm^2
	Interchangeable weights allow pressure to be adjusted as required.
Max. measuring voltage	2000V

The cell may be heated up to 150°C by means of two heating plates. It can be evacuated to permit measurements in an inert atmosphere. Impregnation of the paper can also be carried out.

Material (high-tension and measuring electrodes and guard-ring):
stainless steel 31

Dimensions	310 mm dia. x 440 mm high
Total net weight	about 35 kg

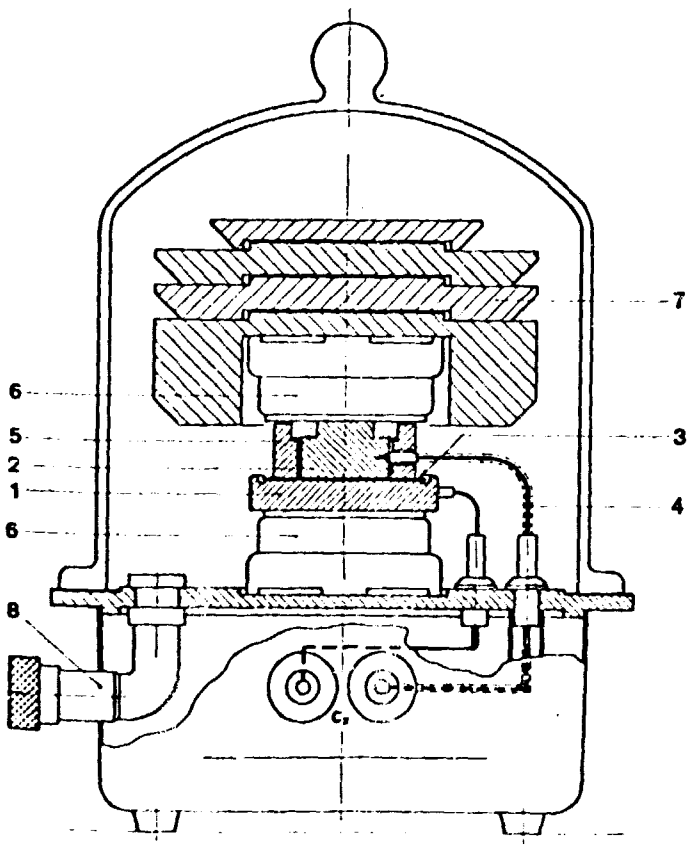

Basic circuit diagram

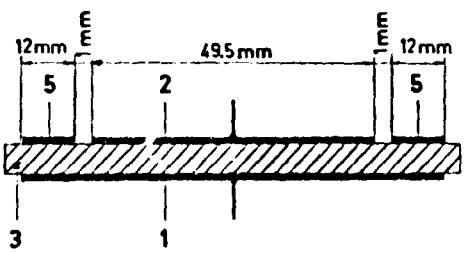

Key

1. High-tension electrode with platinum temperature senser
2. Measuring electrode with platinum temperature senser
3. Testpiece
4. Measuring electrode connection
5. Guard-ring
6. Heater
7. Weights
8. Vacuum connection

TEST ELECTRODE SYSTEMS

General Considerations

The measurement of tanδ, capacitance and complex dielectric constants are based upon measurements with the specimen of the material placed in an electrode system, whose vacuum capacitance can be either accurately calculated or measured in the absence of the test specimen. Therefore, the problem is mainly of determining the two capacitance values accurately, either by calculation or indirectly by comparison with a capacitance standard whose capacitance is accurately known.

Fig (8) shows an electrode system consisting of two parallel plate electrodes, between which the unknown material is to be placed for measurement. In addition to desired inter-electrode capacitance C_v, the system included also edge capacitance C_e, capacitance to ground of the outside face of electrode C_g. It becomes necessary, then, to eliminate these undesired capacitances. If one measuring electrode is grounded, as is often the case, all capacitances except the ground capacitance of grounded electrode and its lead are in parallel with desired capacitance. If a guarded test cell is used, the capacitance to ground no longer appears and capacitance at terminals is C_v, C_e and lead capacitance can be made very small.

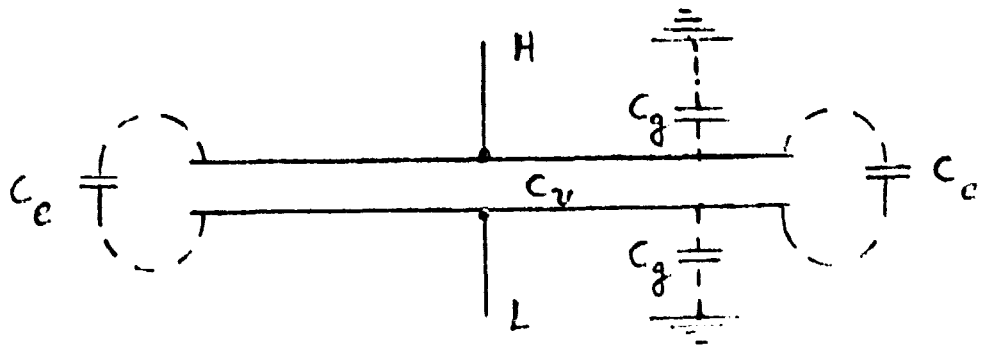

Fig (8)

High Voltage Electrode System and Sample Holder

The high voltage electrode system was designed to measure the variation of tanδ with the changes in temperature, Corona intensity, and electrical voltages. This system shall be capable of performing satisfactorily in the temperature range or -100°F to +450°F and test high voltages up to 10 Kv r.m.s. 60 Hz.

For the purpose of this experiment, the three terminal method was selected. Guarded electrodes arrangement is considered to be quite an accurate method because it involves the least corrections. No edge capacitance or fringing and stray capacitance appears in the results. Ground capacitance is also made to zero.

The electrode system consists of two circular disc type electrodes with a guarding ring electrode. The insulating material under investigation is placed between the electrodes

as shown schematically in Fig (9).

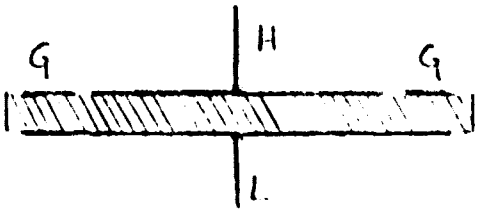

G Guard Ring

Fig (9) Schematic Diagram of Guarded Electrode

Fig (10) shows the details of the electrode system.

The heavy specimen holder consists of electrodes designed to lay cylindrical with the guard ring and guarded electrode in a coaxial arrangement. The cylindrical guard ring and guarded electrode are made of brass and they are separated by a cylindrical tube of teflon. The lower and upper surface of the ring and this electrode are ground to nearly optical flatness. A small hole is made in the outer periphery of the ring and teflon tube up to the inner measuring electrode and a coaxial cable is connected such that one of its wires connected measuring electrode to detector and the other connected guard ring to ground terminal. Teflon cylindrical sheet also maintains a uniform gap between measuring electrode and ring. High voltage electrode, which is below the measuring electrode, is also made of brass and machine ground to perfect flatness. This electrode rests on a cylinder of teflon with an aluminum

base. The high voltage connector enters from the side of the teflon cylinder and is attached to the back surface of the high voltage electrode. The diameter of the high voltage electrode is made larger than the ring.

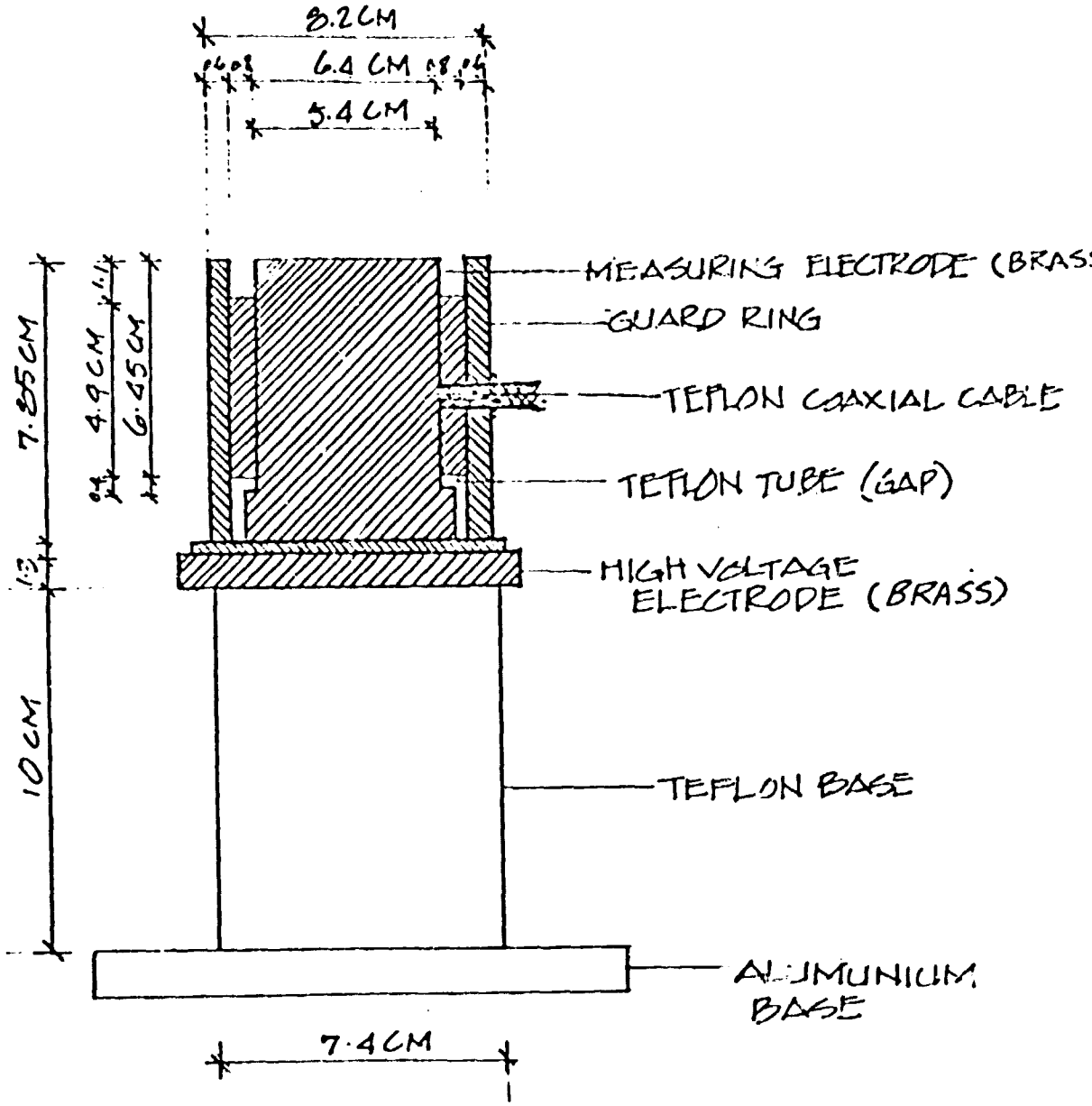

Fig (10). Screened Electrode System for High Voltage Capacitance Measurements.

The whole assembly of the electrode system with a test specimen was put in the test chamber described earlier. High voltage was applied and gradually increased to 10 Kv r.m.s.

Temperature inside the chamber was also varied from $-75^{\circ}F$ and $+400^{\circ}F$; the electrode system performed well. No flashovers or spurious discharges were observed. And the connections and the high voltage systems were tested and found to be Corona free up to 10 KV r.m.s.

This complete system is now ready and calibrated for the measurement of tanδ and dielectric constants of sheet type insulating materials. The measurement of tanδ can be correlated both to the quality and stability of the insulating material under investigation.

Measurement of tanδ and Capacitance at High Frequencies

Measurements will also be made at high frequencies up to 30 MHz. Resonance methods are used to measure both tanδ and capacitance. Fig (11) shows the schematic diagram for the HP 4342A Q Meter used for these measurements. A three terminal guarded micrometer electrode and a two terminal micrometer electrode are used to test the dielectric materials. Fig(13) shows the guarded micrometer electrode. The capacitance standard on the Q meter has calibration accuracy traceable to National

Bureau of Standards. The edge correction for the unguarded electrodes were applied according to ASTM Standards D150.

Fig (12) shows the measurement set-up with the two terminal micrometer electrode.

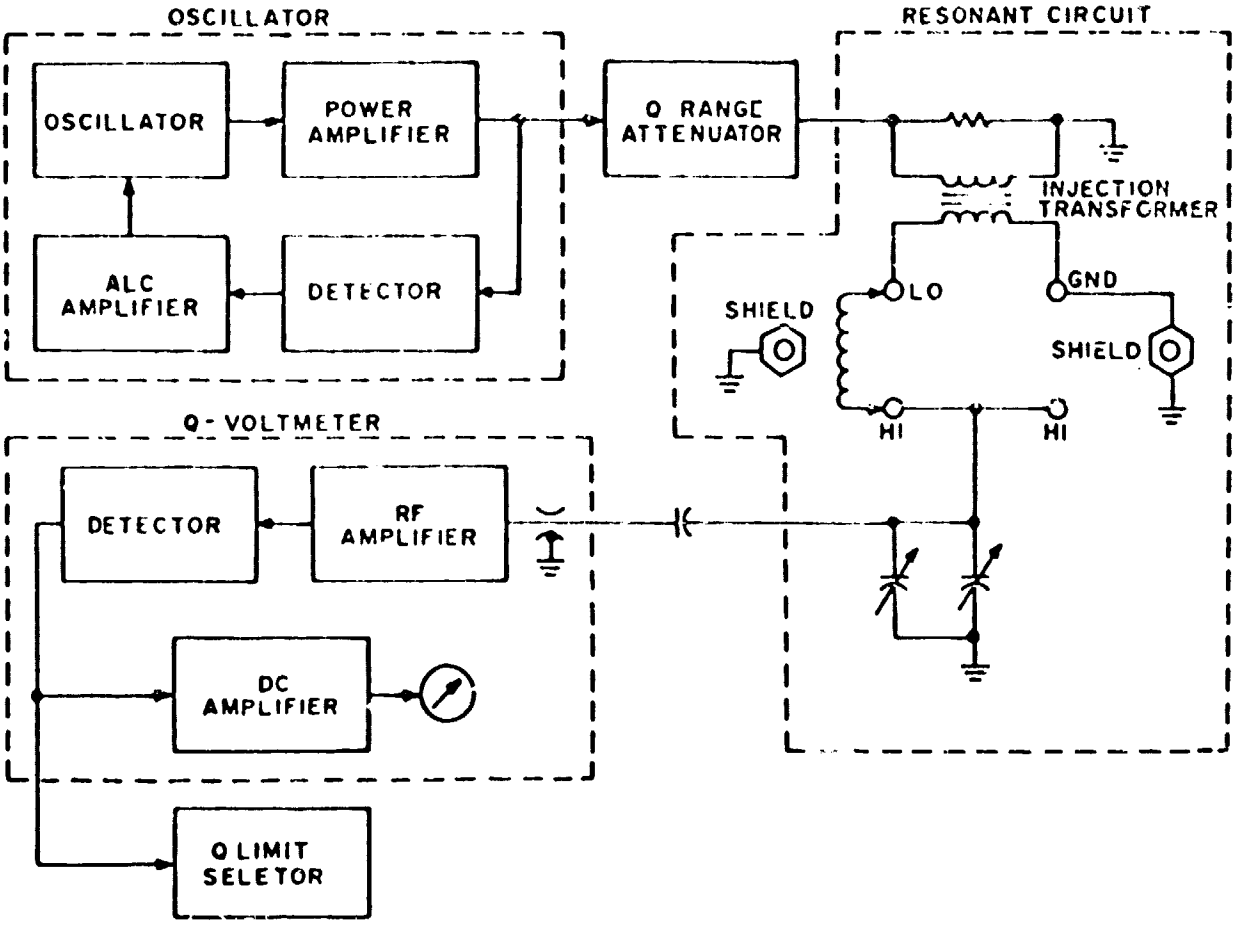

Fig (11) Q Meter Schematic Diagram.

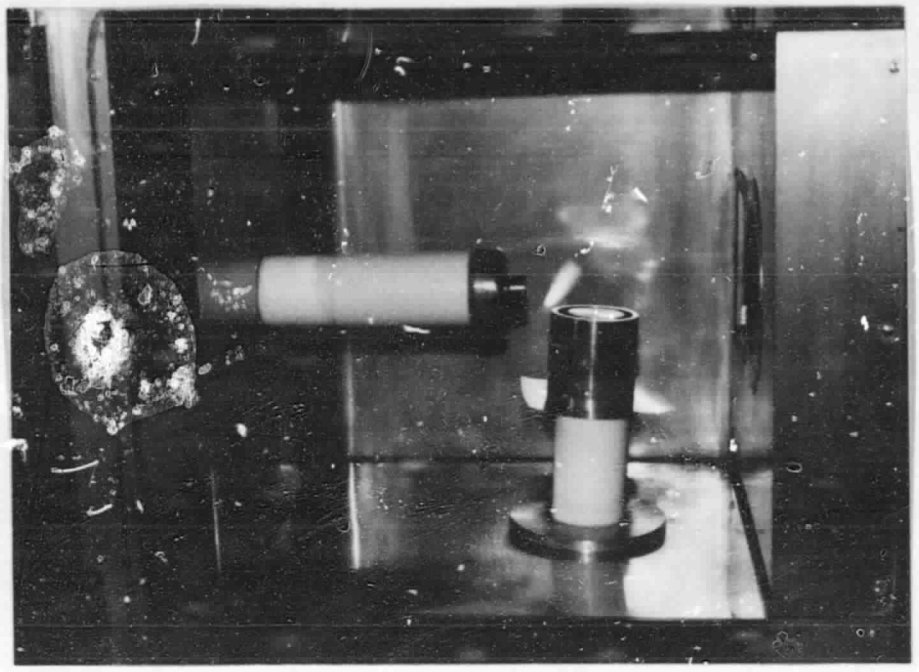

High Voltage Electrode Inside the Test Chamber

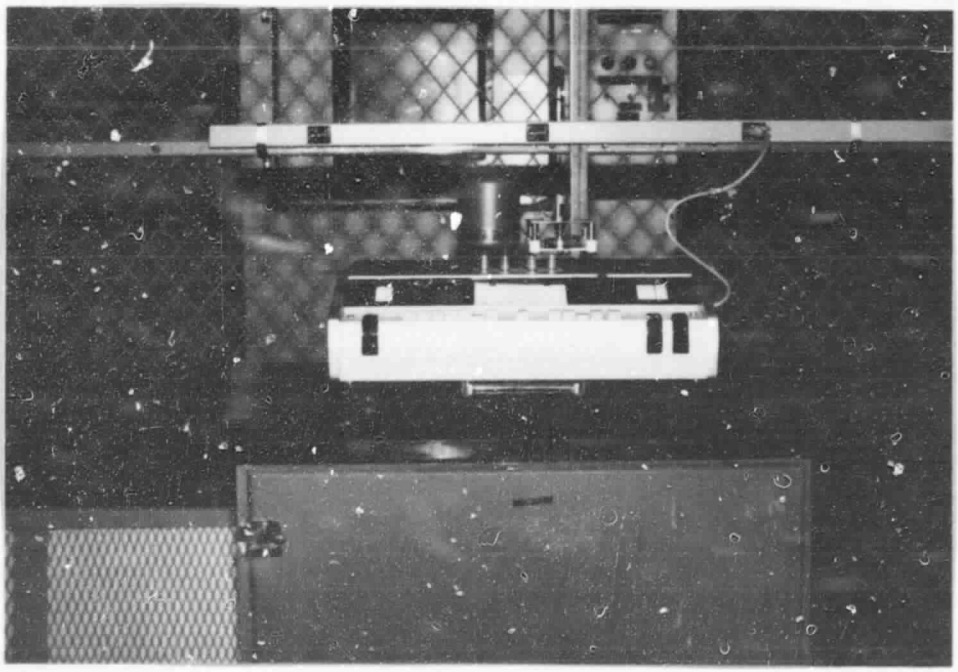

Fig (12) High Frequency Test Set Up

Micrometer Electrodes: Micrometer electrode system was developed to eliminate errors caused by series inductance and resistance of the connecting leads of the measuring capacitor at high frequencies. Fig (13) shows the micrometer electrode system proposed to be used for measurements of tanδ at high frequencies. Carefully calibrated, the micrometer system eliminates the need for corrections for edge and ground capacitances. This electrode system will be used for measurements at the frequency range of 20 KHz - 70 MHz.

Geometry of Specimens: The practical geometrical shapes of electrode systems for which the capacitance can be most accurately calculated are guarded flat parallel plate electrodes and coaxial cylinder electrodes. The equations for calculating the interelectrode capacitances are listed in ASTM STD D-150-70. (19) Flat circular electrodes are generally used for testing Solid Sheet insulating materials whereas coaxial cylindrical electrodes are used for liquid dielectrics. Corrections for stray field edge effects and the effects of the guard gap are made according to the methods described in reference (19). The effective area of the guarded electrode is greater than its actual area by approximately half the area of the guarded gap.

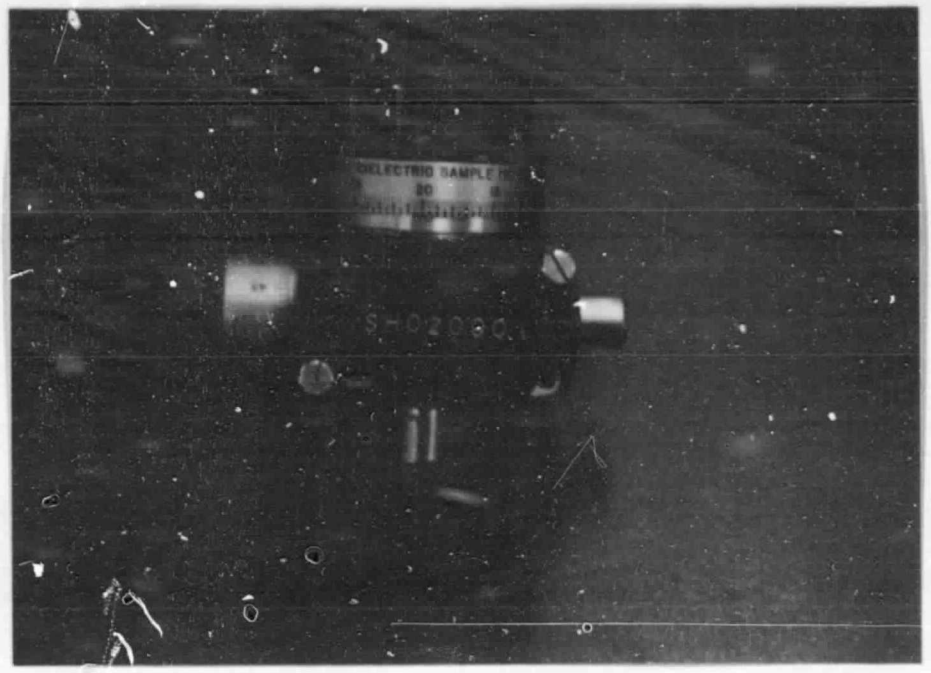

Fig (13) Micrometer Electrode System

Measurement of Volume Resistance

The volume resistivity of the insulating material will change due to two primary reasons:

(1) The heat generated in the material due to leakage currents which may bring about changes in molecular structure. The insulating material may also deteriorate due to external heat sources, mainly from the solar radiation;

(2) The penetration of electrons and ions, present in

the plasma, under the influence of high electric fields.

The principle of measurement of volume resistance consists in measuring the current through the specimen and the voltage across the specimen.

The unknown Resistance $R_x = V_x/I_x$.

However, the measurements must be made keeping in view the following aspects:

(1) Fringing of the lines of current at the guarded electrode edges may effectively increase the electrode dimensions;

(2) Because the insulation resistance of solid dielectric specimens may be extremely high, unless extreme care is taken with the insulation of the measuring circuit, the values obtained may be more a measure of apparatus limitation than the material itself;

(3) Where the test specimen has appreciable capacitance, short-time transients as well as relatively long-time drifts in the applied voltage may cause spurious capacitive charge and discharge currents, which can affect the accuracy of

measurement;

(4) When capacitance is very large, the resistance R_x should be measured by "Voltage Rate of Change Method" as defined in ASTM Standard D257;

(5) If the plane electrodes are not parallel, the current density in the specimen will not be uniform and an error may result. This error is usually small and may be ignored.

Correction to Edge effects and fringing must be applied (19).

Fig (14) shows a circuit for measuring the volume resistance.

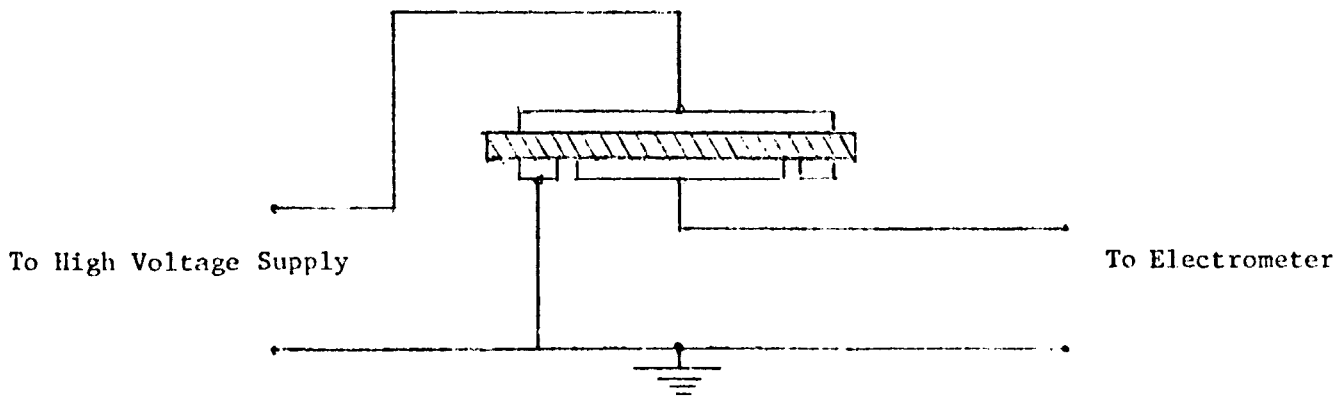

Fig (14)

Schematic Diagram for Volume Resistance Measurements.

Fig (15) shows the experimental set-up for D.C. resistivity measurements at the ambient temperature in air. Low voltage test cell will be used for measurements at higher temperatures, inert atmosphere and vacuum.

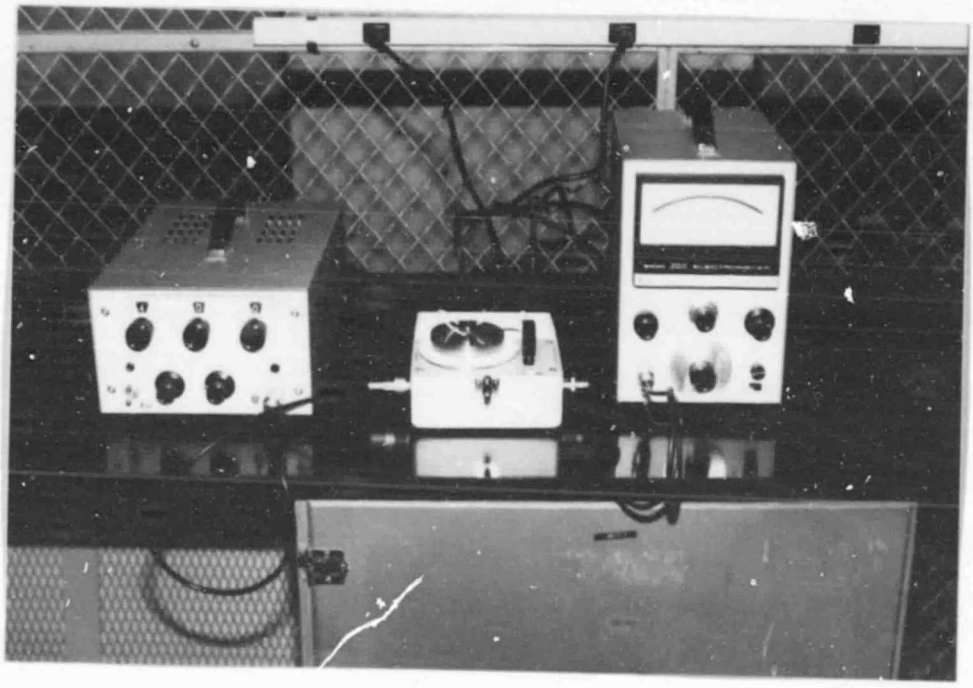

Fig (15) D.C. Resistivity Measurement Set Up

Measurement of Surface Resistance

The surface resistance of the insulating material will change due to the action of charged particles, plasma and surfacing arcing. Chemicals and gases in the environment in which the insulating material is located will also alter the

chemical and molecular structure of the surface of the insulating material, thereby damaging the insulating properties. Fig (16) shows the circuit diagram of the set-up used for measuring the surface resistance. In case of insulating materials used on solar cells, only the effects of plasma interaction and thermal effects are of importance in surface degradation.

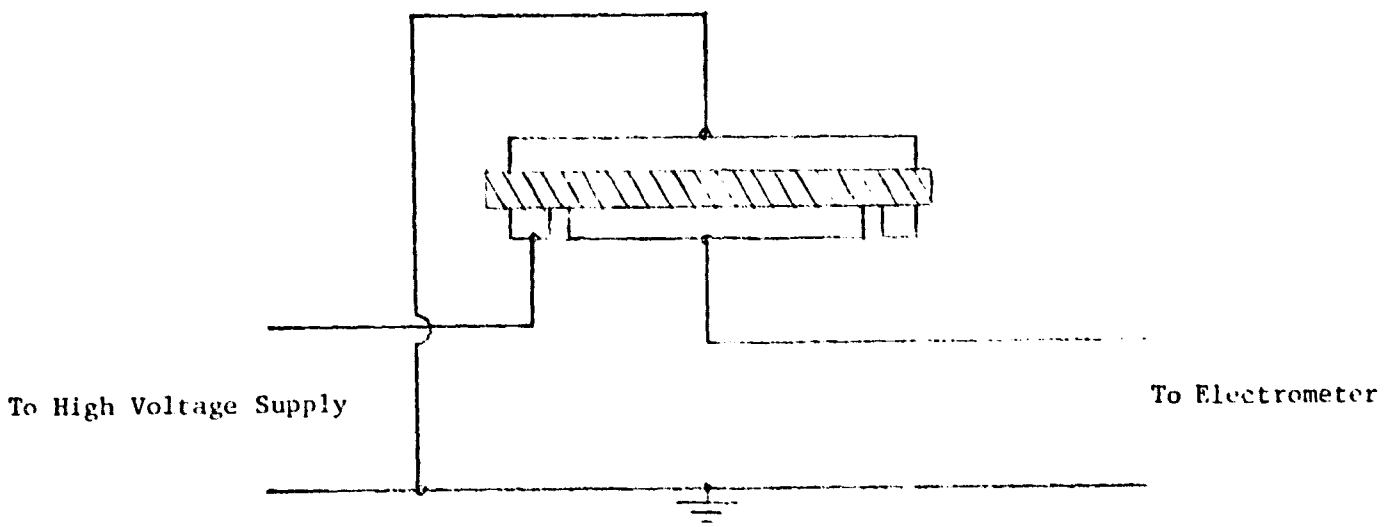

Fig (16) Schematic Diagram for Surface Resistance Measurement.

On thick samples of materials, high voltage low current dry arc test according to ASTM Standard D495 is recommended.

Computation of Volume and Surface Resistivity

Type of Electrodes — Circular with guard ring

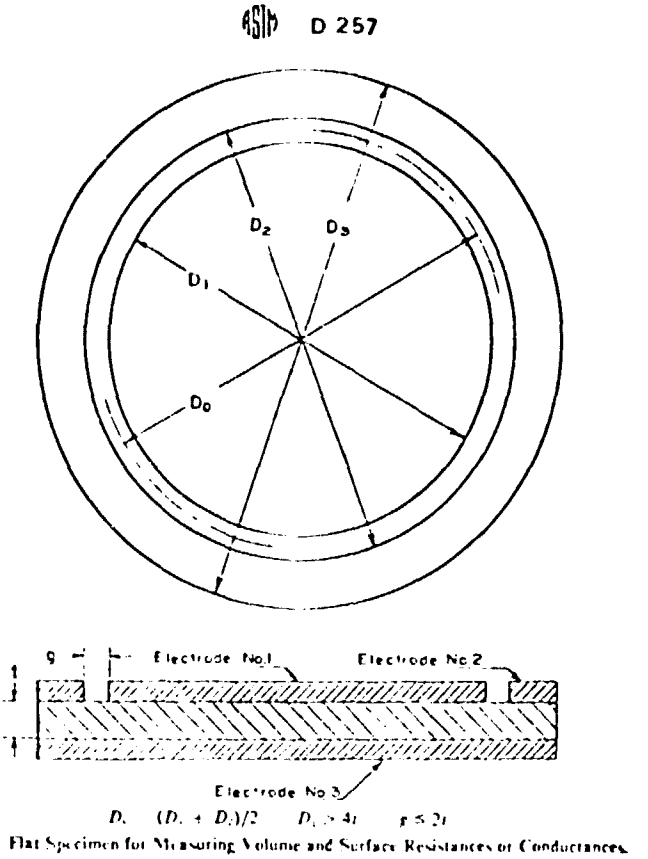

Flat Specimen for Measuring Volume and Surface Resistances or Conductances

Volume resistivity $\rho_v = \frac{A}{t} R_v$. ohm cm.

R_v = Measured volume resistance ohms

t = Average thickness of sample

$A = \frac{\pi (D_1+g)^2}{4}$

Surface resistivity $P_s = \frac{p}{g} R_s$ ohm cm.

R_s = Measured surface resistance in ohms

$p = \pi D_o = \pi (\frac{D_1+D_2}{2})$

g = Guard gap

CHAPTER VI

MEASUREMENT AND INSTRUMENTATION SYSTEMS

The accuracy of measurement of small dissipation factors depends on the constancy of bridge elements and the loss reference Standard Capacitor. The characteristics of the Standard Capacitor used in each type of measurement is specified.

High Voltage Measurements

The measurement of the dissipation factor, and capacitance at high voltages of 0-10 Kv at 60 Hz will be conducted using a high voltage Schering bridge. The loss reference is a Standard Compressed gas (carbon dioxide) Capacitor 100 pF 190 Kv r.m.s. $\tan\delta \leq 10^{-5}$. The Standard Capacitor and the bridge elements used in this measurement are similar to those used in standard laboratories internationally.

The high voltage test chamber will be used to subject the sample to simultaneous thermal and electrical stresses, in air. The chamber will also be used to expose the test sample to corona discharge.

Standard Capacitor Tettex type. 3370/100/190

High voltage Schering Bridge Tettex type. 2801/RQ

Partial Discharge Test Equipment

Partial discharge test equipment (James Biddle Type $66J_b$) will be used to measure the partial discharges. The system can detect partial discharges as low as 0.10 pico coulomb.

Low Voltage Measurements

The measurement of tanδ and capacitance at low voltages at 30 V, 1000Hz will be made using the low voltage test cell. A transformer ratio arm bridge (Gen Rad Type 1615) with a tuned amplifier null detector will be used to measure the capacitance and the dissipation factor. The measurement accuracies are at 1 KHz $\pm$ (0.1% + 0.00003PF) with a resolution least count of 10^{-17}F for capacitance measurements and $\pm$ 0.1% with a least count of 10^{-6} for dissipation factor measurements.

The low voltage test cell will also be used to measure both the D.C. volume and surface resistivities up to 2 Kv D.C. Both A.C. and D.C. tests can be conducted in an inert atmosphere of nitrogen and in vacuum at any required temperature in the range 0-150^{0}C.

D.C. Resistivity Measurements

Both ASTM and VDE Standard electrodes will be used for the D.C. Volume and Surface resistivity measurement. The test voltage values 0-1000V D.C. $\pm$ 1% with a stability of $\pm$ 2 mV

per hour. The electrometer has an accuracy of $\pm$ 4% in the range 3 x 10^{-12} to 10^{-14} amperes full scale. Only VDE Standard electrodes will be used for tests in vacuum (10^{-3} Torr) and in inert atmosphere).

Breakdown Test

Ultimate breakdown tests will be conducted according to ASTM Standard D149-64 (1970). This is a destructive test.

CHAPTER VII

PLANS FOR FURTHER WORK

A comprehensive test and instrumentation system has been developed, checked, and calibrated for insulation research as detailed earlier in this report.

The insulation aging and breakdown process is complex and inherently random in nature. Hence, it is necessary to conduct large numbers of tests under identical test conditions and analyze the results using statistical methods (13,18).

The following test and analysis program will be carried out in the future when adequate number test samples, time and manpower become available:

TEST PROGRAM

(1) Make control measurements on unstressed samples;

(2) Measurements consist of capacitance, tanδ, volume resistivity, and surface resistivity;

(3) Keep temperature constant, measure

(a) tanδ vs. time (in hours)

at various test voltages.

Allow sufficient time until tanδ is essentially

constant, and does not appreciably vary with time;

(4) Keep test voltage constant.

Measure tanδ vs. temperature;

(5) Expose test sample to corona discharge.

Measure the corona current. Repeat tests (3) and (4) with the test sample exposed to corona for specified time;

(6) Measure D.C. volume and surface resistivities for conditions specified in (3), (4) and (5) above;

(7) Apply Standard Statistical methods and analyze the data;

(8) Establish correlation between stress levels, time of exposure, and other various factors to the quality of the insulation as indicated by the dissipation factor and D.C. resistivities.

The changeover from A.C. measurement set-up to D.C. measurement set-up is simple with the system developed. This system is designed to facilitate this changeover with the exchange of a few plug-in connectors and calibrated cables.

CHAPTER VIII

BIBLIOGRAPHY

1. Stern, J.E. and Mercy, K.R. "Study of Voltage Breakdown in Spacecraft Systems from Test and Flight Experience." IEEE TRANS EL Insulation Vol. El 6 No. 2, June 1971 90-93.

2. Forsberg, K. "Final Report on Corona/Voltage Breakdown Survey" NASA Contract 5-11593 Dec. 2, 1968.

3. Mercy, K. "Survey and Analysis of Voltage Breakdown Problems Associated with Space Problems." T & E Div. Goddard Space Flight Center, Greenbelt, Maryland, 1967-1969 PEP Rep 102 Feb. 1968.

4. A Manual for the Prevention of Electrical Breakdown in Spacecraft, NASA Sp 208.

5. Dunbar, W.B. "Corona Onset Voltage of Insulators and Bare Electrodes in Rarefield Air and Other Gases," AFAPL TR 65-122 June 1966.

6. Paul, F.W. and Burrowbridge, D.R. "Prevention of Electrical Breakdown in Spacecraft." IEEE Trans on El Insulation Vol. El 6 No. 3, September 1971 114-124.

7. Stevens, J.N. "Solar Array Experiments with the Sphinx Satellite," 1973, NASA TMS - 71458.

8. Kennerud, K.L. "High Voltage Solar Array Experiments," NASA LEWIS RESEARCH CENTER - BOEING COMPANY, Report No. CR121280, 1974.

9. Lockheed-MSFC Report #LMSC D 492670, July 1976.

10. Lockheed-MSFC Report #D492657 - April 1976.

11. Coelho, Roland. Physics of Dielectric for the Engineer. Elsevier Scientific Publishing Company (1979).

12. Paul, F.W. and Burrowbridge, D.R., "Prevention of Electric Breakdown in Spacecraft," IEEE Trans on El Insulation Vol. El 6 No. 3 September 1971 114-124.

13. Goba, F.A. Bibliography on "Thermal Aging of Electrical Insulation," IEE Trans El. 4 No. 2, June 1969.

14. Densley, R.J. and Salvage, B. "Partial Discharges in Solid Dielectrics under Impulse Voltage Conditions," IEEE Trans El Insulation El 6 No. 2, June 1971 - 54-72.

15. Van Lint, V.A.J. and Harrity, J.W. "Ionization Radiation Effects on Insulators and Insulating Parts," IEEE Trans on El Insulation Vol El 6 No. 3, 111-113.

16. Simoni, L. "A New Approach to the Voltage Endurance Test on Electrical Insulation," IEE Trans on El Insulation Vol. El 8 No. 3, 76-86, September, 1973.

17. Watson, D.B.W., Heyes, K.C. Kao, and P. H. Calderwood, "Some Aspects of Dielectric Breakdown in Solids," IEEE Trans. El Insulation Vol. EI-7 November, 1965, 30-37.

18. Statistical Analysis of Thermal Life Test, Guide for the, (IEEE Std 85-1973) (SH 0051).

19. ASTM,"American Standard Methods of Test for A.C. Loss Characteristics and Dielectric Constand of Solid Electric Insulating Materials." ASTM Standard D-150 (1970).

20. Sillars, R.W. "Electrical Insulating Materials and Their Applications", IEE Monograph Series No. 14, Peter Peregrinus, 1973.

21. Saums, H.L. and Pendleton, W.W. "Materials for Electrical Insulating and Dielectric Functions." Haydon Book Co., 1973.

22. Tareev, B. "Physics of Dielectric Materials. Mir Publishers, Moscow, 1975.

23. Bruins, P. "Plastics for Electrical Insulation," Wiley.

24. Simioni, L. "A General Approach to the Endurance of Electrical Insulation under Temperature and Voltage," IEEE Trans Electrical Insulation, Vol. EI16, #4, pp. 277-289,Aug,1981

25. Kelen, A. "Aging of Insulating Materials and Equipment Insulation in Service and Tests." IEEE Trans Electrical Insulation, Vol. EI-12-#1, pp. 55-60, February, 1977.